Biotechnology Reports 51 (2026) e00966

Contents lists available at ScienceDirect

Biotechnology Reports

journal homepage: www.elsevier.com/locate/btre

Research Article

Dissection of MAPK and NF-κB p65 signaling dynamics underlying LPS tolerance in macrophages at the single-cell level

Tuntikorn Laosuk [a], Patipark Kueanjinda [b], Hiroshi Kimura [c,d], Tanapat Palaga [e,f,*]

[a] Program in Biotechnology, Faculty of Science, Chulalongkorn University, Bangkok 10330 Thailand
[b] Department of Pathology, Faculty of Medicine, University of Massachusetts Chan Medical School, Worcester, MA 01655 USA
[c] Graduate School of Bioscience and Biotechnology, Institute of Science Tokyo, Midori-ku, Yokohama, Kanagawa 226-8501 Japan
[d] Cell Biology Center, Institute of Innovative Research, Institute of Science Tokyo, Midori-ku, Yokohama, Kanagawa 226-8501 Japan
[e] Center of Excellence in Immunology and Immune-mediated Diseases, Chulalongkorn University, Bangkok 10330, Thailand
[f] Department of Microbiology, Faculty of Science, Chulalongkorn University, Bangkok 10330, Thailand

ARTICLE INFO

Keywords:
LPS tolerance
Macrophages
ERK
NF-κB
Signaling dynamics

ABSTRACT

MAPK and NF-κB pathways regulate macrophage responses to microbial stimuli. Repeated exposure to lipopolysaccharide (LPS) induces endotoxin tolerance, a state in which inflammatory cytokine production is suppressed while antimicrobial functions are preserved. Although regulatory mechanisms of LPS tolerance is well established, how prior LPS exposure reshapes signaling dynamics downstream of TLR4 remains unclear. Using biosensors and live-cell imaging, we quantified ERK and NF-κB signaling in RAW264.7 macrophages during LPS tolerance. Tolerized macrophages produced less TNF-α and IL-6 and showed reduced ERK and NF-κB activity, with lower amplitudes and areas under the curve than cells receiving a single LPS stimulation. Both pathways also displayed delayed activation, reflected by a prolonged time to first peak. Inhibition experiments revealed bidirectional crosstalk, as blocking ERK altered NF-κB signaling and NF-κB inhibition suppressed ERK dynamics. These findings show that LPS tolerance involves coordinated changes in the strength and timing of ERK and NF-κB signaling.

1. Introduction

The innate immune system is the first line defense mechanism against infections [1]. It has long been known that only adaptive immunity has memory that mediates effective response to repeated exposure to the same pathogens. Recently, evidences show that innate immunity also possesses memory [2]. Innate immune memory manifests as either tolerance or trained immunity, whereby innate immune cells exhibit altered responses upon re-stimulation with unrelated stimuli compared with the initial exposure. Innate immune memory is mediated in part by metabolic reprogramming and epigenetic modifications that influence the expression of genes involved in inflammatory response [3]. Innate immune memory is reported in various types of innate immune cells, including monocytes, macrophages, natural killer cells and innate lymphoid cells [4].

Endotoxin tolerance refers to the diminished inflammatory responsiveness of innate immune cells, particularly macrophages and monocytes, upon repeated stimulation with bacterial endotoxin [5]. Lipopolysaccharide (LPS), is a well-characterized pathogen-associated molecular pattern (PAMPs) that induces strong inflammatory responses via the pattern recognition receptors (PRRs), Toll-like receptor 4 (TLR4). Engagement of LPS with the CD14–TLR4 complex triggers an acute inflammatory response characterized by rapid and robust production of pro-inflammatory cytokines, as well as the induction of additional effector functions, including antimicrobial molecules [6]. Upon re-stimulation with LPS or other PAMPs, macrophages enter a tolerant state characterized by attenuated inflammatory responses while antimicrobial effector functions are preserved [7]. The interval between the first and second rounds of stimulation is critical, as it permits cellular recovery and the restoration of activated signaling pathways to baseline levels prior to the second encounter [8].

The signaling pathways involved in primary activation through LPS/CD14/TLR4 are well characterized, especially the key signal pathways via the mitogen-activated protein kinase (MAPK) and NF-κB pathways. In contrast, the mechanisms underlying LPS re-stimulation–induced tolerance remain incompletely understood [9]. Successive LPS

* Corresponding author at: Center of Excellence in Immunology and Immune-mediated Diseases, Chulalongkorn University, Bangkok 10330, Thailand.
E-mail address: tanapat.p@chula.ac.th (T. Palaga).

https://doi.org/10.1016/j.btre.2026.e00966
Received 11 February 2026; Received in revised form 27 May 2026; Accepted 7 June 2026
Available online 8 June 2026

stimulation attenuates downstream signaling events, including MyD88–TLR4 association, activation of NF-κB and MAPK pathways, and IκBα degradation[9]. The reduction of downstream TLR signaling causes dampened pro-inflammatory cytokine production [10]. In sepsis patients, LPS tolerance plays important roles in preventing severe tissue injuries due to massive cytokine productions but preserve anti-microbial functions [11]. However, prolonged LPS tolerance may progress to immune paralysis, thereby increasing susceptibility to secondary infections and adverse clinical outcomes, including increased mortality [10,12,13].

Extracellular signal-related kinases 1 and 2 (ERK1/2) are elements in the MAPK pathway that play important roles in, for example, cell growth and cell survival downstream of TLR4 [14]. On the other hand, the NF-κB pathway also plays vital functions in an inflammatory response that transmits the signal from surface receptor TLR4 to regulate key pro-inflammatory and anti-microbial related gene expression upon infections. The inflammatory responses initiated by both pathways drive the expression of pro-inflammatory cytokines, including tumor necrosis factor-α (TNF-α) and interleukin-6 (IL-6), via the activation of transcription factors such as AP1 in the ERK1/2 pathway and p65/p50 in NF-κB activation [14–16].

The signal transduction and the dynamics of NF-κB during activation in macrophages have been documented [17–21]. To elucidate the signaling dynamics, the MAPK sensor and NF-κB reporters were developed to track signaling oscillation in stimulated cells [22,23]. Both MAPK and NF-κB signaling pathways in macrophages display dynamic response patterns during bacterial infection [24]. Wang et al. reported a microfluidic-based compound screening platform that induced LPS tolerance in macrophages, revealing innate immune memory dynamics mediated by NF-κB signaling pathways [25]. In the studies of the transcriptomic and epigenetic profiles of LPS tolerance and inhibitor screenings, the results convincingly demonstrated the involvement of metabolic reprogramming and epigenetic reprogramming [7,26–28]. Furthermore, detailed signaling investigation identified PI3K, Akt, and phosphatase SHIP1 as important regulators of endotoxin tolerance [29]. Although MAPK and NF-κB signaling pathways have been extensively studied in response to acute LPS stimulation, detailed analyses of their dynamic regulation during LPS tolerance, particularly at high temporal and single-cell resolution, remain limited.

In this study, we dissected the signaling dynamics of the ERK1/2 MAPK and NF-κB p65 pathways during LPS tolerance, in comparison with LPS priming, using RAW264.7 macrophages stably expressing an NF-κB p65 reporter and an ERK1/2 kinase translocation reporter (KTR) sensor [23]. The cross-regulation of these two keys signaling pathways were also examined using specific inhibitors. Because endotoxin tolerance depends on prior LPS exposure, studying how key signaling pathways change over time is crucial for understanding how inflammation is restrained while antimicrobial functions are preserved. Defining how signaling dynamics are rewired during LPS tolerance may inform strategies to prevent immune paralysis while preserving host defense in conditions such as sepsis and chronic infection.

2. Material and methods

2.1. Plasmids preparation

The reporter plasmids, ERK1/2 kinase translocation reporter (pLentiCMV Puro DEST ERKKTR Clover) and NF-κB p65 reporter (pLenti_Blast_DESTmouse_p65promoter_mouse_p65-mRuby2), were obtained from Addgene, USA (catalog numbers #59150 and #124903, respectively).The NF-κB p65-mRuby2 reporter was constructed as a C-terminal fusion, where the mRuby2 fluorescent protein was linked to the C-terminus of the mouse NF-κB p65 protein. The Histone 2B reporter was obtained by combining pCDH-CMV-MCS-EF1-Hyg and PB533_H2B-Halo. For packaging plasmids, the 2nd generation lentivirus packaging plasmid consisting of psPAX2 and pMD2.G were used (Addgene, USA). All plasmids were prepared and purified by the ZymoPure II plasmid midiprep kit (Zymo Research, USA).

2.2. Generation of stable reporter cell line

Reporter constructs in lentiviral plasmids were transfected into the HEK293T cell line together with the 2nd generation packaging plasmids using Lipofectamine 3000 (Thermo Fisher Scientific). The packaged lentivirus was used to perform spinfection (2200 rpm for 30 min) using 8 μg/ml polybrene to RAW264.7 (ATCC TIB-71^{TM}). The transduced RAW264.7 was rested for 24 h prior to a drug selection using blasticidin (6 μg/ml) for 3 days. RAW264.7 cells stably expressing NF-κB p65 reporter was sorted by fluorescence activating cell sorter (FACS) and subjected to serial transduction with the lentiviral plasmids for histone 2B Halo and ERK KTR. The stable reporter cell line was selected by hygromycin B (140 μg/ml) and puromycin (4 μg/ml) and further sorted by FACS. All cell lines in this study were maintained in Dulbecco's modified Eagle's medium (DMEM, HyClone, USA) augmented with 10% (v/v) fetal bovine serum (Gibco, USA), 1% (w/v) of sodium pyruvate, 1% (w/v) of HEPES, and 100 U/ml penicillin/streptomycin.

2.3. Enzyme-linked immunosorbent assay (ELISA) for IL-6 and TNF-α

The stable reporter cell line was seeded at 1×10^4 cells per well in 96-well plates for 16–18 h before stimulation. After LPS stimulation or repeated LPS stimulation (LPS tolerance) as indicated, the culture supernatants were harvested to assess cytokine production. IL-6 and TNF-α levels were quantified using mouse IL-6 ELISA and TNF-α ELISA kits (BioLegend, USA) in accordance with the manufacturer's instructions. Absorbance at 450 and 620 nm was measured by a microplate reader (Thermo Fisher Scientific).

2.4. Reverse transcription-quantitative polymerase chain reaction (RT-qPCR)

The stable reporter cell line was harvested after 3 h of LPS stimulation or repeated LPS stimulation, and the total RNA was collected by TRIzol (Invitrogen, USA) by following the manufacturer's protocol. The extracted RNA was treated with DNase by RQ1 RNase-free DNase (Promega). Treated RNA was cleaned up in an RNeasy Mini Kit (QIAGEN, USA). Hundred nanograms of total RNA were converted to cDNA by using SuperScript III reverse transcriptase, random hexamer (Thermo Fisher Scientific), dNTP mix (Takara Bio, Japan), and RNaseH (Thermo Fisher Scientific) and the obtained cDNA was treated again with the MinElute PCR Purification Kit (QIAGEN, USA). The purified cDNA was combined with PowerUp SYBR Green Master Mix (Thermo Fisher Scientific) and specific primers (Table 1). The qPCR was performed with Mx3000P (Agilent Technology). The $2^{-\Delta\Delta ct}$ method was used to normalize the data with *Gapdh*.

2.5. Live-cell imaging

RAW264.7 stable reporter cell line was seeded at 1×10^5 cells in the 8-well chambers (MATSUNAMI, Japan) in 10% FBS DMEM. To synchronize cells, the media 10% FBS DMEM was replaced with 1% FBS

Table 1
List of primers utilized in this research.

Gene name	sequence	reference
Tnf	F: 5′- ACCCCTTTATTGTCTACTCCTC-3′ R: 5′- GTCCCAGCATCTTGTGTTTC-3′	[30]
Il6	F: 5′- CAGAAACCGCTATGAAGTTCC-3′ R: 5′- CTCTGTGAAGTCTCCTCTCC-3′	This study
Gapdh	F: 5′- TCGGTGTGAACGGATTTG-3′ R: 5′- GGTCTCGCTCCTGGAAGA-3′	[31]

DMEM six hours before the imaging session. For nuclear labeling, 2 nM Janelia Fluor 646 Halo Tag Ligand (Promega, USA) was added to bind with H2B Halo one hour before the start of the imaging session. Cells were washed with 1X phosphate buffer saline (PBS) and replaced with 10% FBS DMEM. Images of the cell were collected according to the indicated stimulation and imaging timelines (Fig. 2**A**). The temperature and humidity of cell cultures were strictly controlled by a control system (Tokai Hit, Japan) to be under 37 °C. The carbon dioxide was used at 5%, which was controlled by a CO_2 control system (Tokken). Heat, humidity, and gas were installed in the confocal microscope (Nikon Eclipse Ti), which operated under fusion software (ANDOR, Oxford Instrument). All images were acquired using a 100x/1.4 oil immersion objective lens with a resolution of 1024 × 1024 pixels. A multi-field procedure was utilized, incorporating 488-nm, 561-nm, and 637-nm lasers to excite Clover, mRuby2, and HaloTag-JF646, respectively. Laser intensities were set at 30%, 30%, and 20% with an exposure time of 300 ms. For overnight live-cell imaging, an autofocus called a perfect focus system (PFS) was used to avoid focus drift. A previous study has reported that LPS-stimulated macrophages' MEK/ERK phosphorylation starts from 5 min to reach 15 min [32], and then we decided to collect image data at the first hour with 5-min intervals. For the imaging session of twenty-three hours, the time interval was changed from a 5-min to a 10-min interval to prevent the effect of phototoxicity. The capture strategies were baseline (4 frames, 5 min interval), 1-h experiment (12 frames, 5 min interval), and 23-h overnight experiment (140 frames, 10 min interval).

2.6. Image processing

An image file from a confocal microscope was processed in the ImageJ v1.54p software (USA) to convert it into an 8-bit with .tif format. To enhance H2B tracking performance, we used StarDist2D in ImageJ to detect the nucleus before tracking and cell segmentation. For file names, the tif file images were converted to the name format 001001-1-001001001, representing row, column, field, time, plane, and channel, respectively. This study only focused on the last three digits, which were 001 for ERK or NF-κB p65 and 002 for H2B. Converted files were used to track the cells using custom MATLAB R2024b (MathWorks) from Heng's CellTracking open source [33]. Tracking data was exported into an .h5 file. For cell segmentation and object quantification, the CellProfiler (USA), an open-source software for cell analysis, was utilized [34,35]. To accurately resolve individual cells within high-density populations, the seeded-watershed approach was employed. The nucleus (primary object) was defined by using the H2B-fused fluorescent protein signal to conduct single-cell segmentation using a global Otsu thresholding method combined with a clump-splitting algorithm to distinguish touching nuclei. To facilitate the quantification of fluorescence intensities across all imaging channels, a cytoplasmic ring (cytoring) was subsequently generated around each nucleus, with a fixed width of five pixels [23]. This secondary segmentation was achieved by expanding the nuclear outlines using a distance-based propagation algorithm, which effectively defines cellular boundaries even when cells are in close proximity by preventing the merging of adjacent cytoplasmic regions. The image data from quantification, such as mean intensity of cytoring and nucleus and cell coordination, were used to calculate the ratio. Both tracking and segmented information were matched by image number and XY coordinates in RStudio Desktop v4.3.1. The matched data were transformed to cytoplasm/nucleus ratio (ERK activity) and nucleus/cytoplasm (NF-κB activity). Activity data was normalized by subtracting the average of 4 time points (20 min at baseline, 4 time points, 5 min each) before stimulation from every data point (Fig. 2**A**).

2.7. Single-cell signaling feature quantification

ERK and NF-κB activity was quantified as the signaling feature that was composed of area under the curve (AUC), time to first peak, and amplitude. AUC was defined as the sum of the C/N or N/C ratios from the time points 5 onward, corresponding to 20–380 min (6 h) post-stimulation for the early overnight experiment period. The time to first peak was determined as the interval between LPS administration and the first identified signaling maximum. Peaks were identified using the findpeak function in the R package. They could also be manually identified based on their slope and relative amplitude thresholds. The relative amplitude threshold was defined as the C/N or N/C ratio of a cell at a given time point that exceeded the average C/N or N/C ratio after stimulation within the same experiment. Individual signaling features from each cellular response were visualized using violin plots to compare responses between single LPS stimulation and LPS tolerance conditions.

2.8. Analysis of cross-inhibition quantification

Cross-inhibition activity was determined by subtracting the control activity (mock treatment in LPS tolerance) from the activity of the inhibitor effect (inhibitor with LPS tolerance) as described by Miura *et al.* [36]. For a schematic of quantification in terms of $\triangle$NF-κB $_{\text{Tolerance}}$, $\triangle$NF-κB $_{\text{ERK inhibitor}}$, $\triangle$ERK $_{\text{Tolerance}}$, and $\triangle$ERK $_{\text{NF-κB inhibitor}}$, the details are shown in Fig. 4**D, E**.

2.9. Statistical analysis and data reproducibility

For statistical analysis, an unpaired Mann-Whitney U test and one-way ANOVA were performed, with the Mann-Whitney U test used for signaling features (BioRender) and one-way ANOVA (multiple comparisons) used for all graphs (PRISM GraphPad). All experiments were performed at least in three biological replicates with two independent experiments.

3. Results

3.1. Dampened IL-6 and TNF-α production upon repeated LPS stimulation (LPS tolerance) in RAW264.7 Trio reporter cell

To accurately monitor signaling dynamics during LPS tolerance, we constructed RAW246.7 Trio that stably expressed NF-κB p65 mRuby2, ERK kinase translocation (KTR) Clover, and H2B Halo Tag for nuclei tracking. To establish LPS tolerance, RAW264.7 Trio cells were first stimulated with 100 ng/mL LPS for 24 h, allowed to rest for 24 h, and subsequently re-stimulated with 10 ng/mL LPS (Fig. 1**A**). Cytokine production was assessed by measuring TNF-α and IL-6 levels in the culture supernatants using ELISA, and responses to repeated LPS exposure were compared with those from a single LPS stimulation. Consistent with the induction of LPS tolerance, repeated LPS stimulation significantly decreased IL-6 and TNF-α productions compared with cells exposed to a single 10 ng/mL LPS stimulation (Fig. 1**B, C**; $p < 0.05$).

Next, RT–qPCR was performed to quantify *Il6* and *Tnf* mRNA levels. Consistent with the ELISA results, repeated LPS stimulation significantly reduced the transcript levels of both *Il6* and *Tnf* compared with cells exposed to a single 10 ng/mL LPS stimulation ($p < 0.05$) (Fig. 1**D, E**). Collectively, these findings demonstrate that the RAW264.7 Trio reporter cell line established in this study can be successfully rendered LPS-tolerant through repeated LPS stimulation. The effect of LPS restimulation on cell viability was tested using MTT and the results showed that repeated LPS stimulation did not affect cell viability compared to untreated cells or cells with single LPS exposure (**Supplementary Figure S1A, B**). Thus, this stimulation scheme will be used to study signaling dynamics in further experiments.

3.2. Dynamics of ERK and NF-κB p65 response during LPS stimulation and re-stimulation

Next, the signaling dynamics in RAW264.7 Trio were monitored

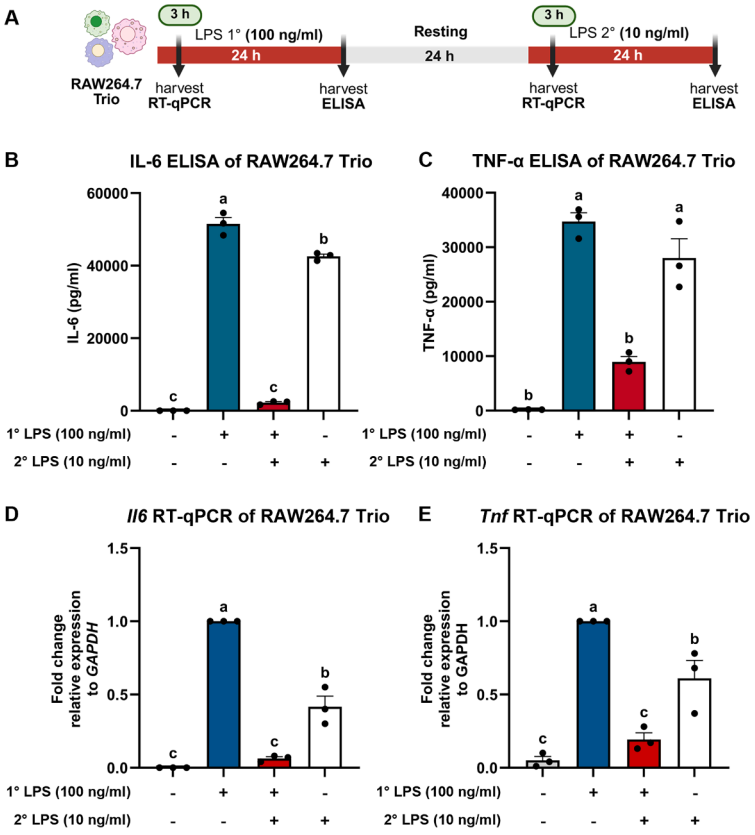

Fig. 1. Stimulation scheme and cytokine responses during LPS priming and re-stimulation (LPS tolerance) in RAW264.7 Trio reporter cells
(A) Schematic illustration of LPS stimulation and re-stimulation in RAW264.7 Trio reporter cells. **(B-C)** Levels of IL-6 and TNF-α in the culture supernatant were measured by ELISA at 24 h after LPS stimulation or re-stimulation **(D-E)** The mRNA levels of *Il6* and *Tnf* was measured by RT-qPCR at 3 h after stimulation or re-stimulation with LPS. Different letters (a, b, and c) indicate statistically significant differences among groups, as determined by one-way ANOVA ($p < 0.05$).

during single LPS stimulation (LPS 1°) for the duration of 24 h. In the absence of stimulation, the ERK KTR–Clover biosensor was predominantly localized in the nucleus. Upon LPS treatment, the sensor rapidly translocated from the nucleus to the cytoplasm. In contrast, NF-κB–mRuby2 was primarily cytoplasmic under resting conditions and translocated to the nucleus following LPS stimulation (**Supplementary Movie**). The experimental timeline was stated in the materials and methods (Fig. 2**A**).

3.2.1. *NF-κB response*

To assess the NF-κB signaling dynamics, reporter activity was quantified as the ratio of nuclear to cytoplasmic fluorescence (N/C). The NF-κB p65 dynamic profile revealed two distinct peaks immediately following LPS stimulation under both single-dose LPS exposure and LPS-tolerant conditions (Fig. 2**B**). The peaks were rapidly induced and declined to baseline by 3 h. The amplitudes of both peaks differed markedly between primary LPS stimulation (LPS 1°) and LPS tolerized conditions (LPS 2°). Single-cell responses visualized as heatmaps revealed that cells contributing to the second peak were more distinct and formed tighter clusters under primary LPS stimulation (LPS 1°) than under LPS tolerized conditions (LPS 2°) (Fig. 2**D, E**, left panel).

3.2.2. *ERK response*

As shown in Fig. 2**C**, the results indicated that the signal was clearly activated with the LPS 1° 10 ng/ml and subsequently decreased after 5 h. In LPS tolerance groups, ERK response was similarly elevated as in LPS 1°, but the activity was swiftly blunted after 3 h (Fig. 2**C**). To monitor the single-cell response in ERK pathway, the data were extracted and presented into a heatmap as one cell response in terms of cytoplasm/nuclear (C/N) intensity ratio. The comparison of a heatmap at LPS 1° and LPS tolerance revealed that there were small cluster of cells with sustained reporter signaling in LPS tolerance than LPS 1° (Fig. 2**D, E**, right panel) that was presented in the middle row of the figure. This result confirmed that repeated LPS exposure altered ERK activation, which was more attenuated and heterogeneous than that observed with primary LPS stimulation, yet still showed ERK activity.

To investigate the coordination between NF-κB and ERK signaling, we generated paired time-series heatmaps. The individual cell was sorted on its NF-κB p65 activity, and the same order was applied to the ERK signaling dataset. The result indicates that while both pathways were concurrently activated in response to LPS or LPS restimulation (tolerance), they exhibited distinct and uncoupled signaling patterns at the single-cell level. For example, the strong activation population of NF-κB did not necessarily display ERK responses that were proportionally or directionally correlated (Fig. 2**D, E**). This paired visualization shows that although these two pathways are co-triggered by the same stimulus, their signaling activation appeared to be controlled by separate regulatory mechanisms. The signaling behaviors exhibited throughout the population are notably diverse and non-patterned within the cell population.

3.3. *Characteristic features of ERK and NF-κB p65 signaling dynamics during primary LPS stimulation and LPS tolerance*

To quantitively compare the difference between LPS stimulation (LPS 1°) and LPS tolerance, we processed the activity data (Fig. 2**B and C**) to extract key signaling features. The signaling features included the area under the curve (AUC), amplitude, and time to first peak. The AUC represents the overall signaling response to the stimulus (LPS in this study). Amplitude denotes the maximal response observed, whereas the

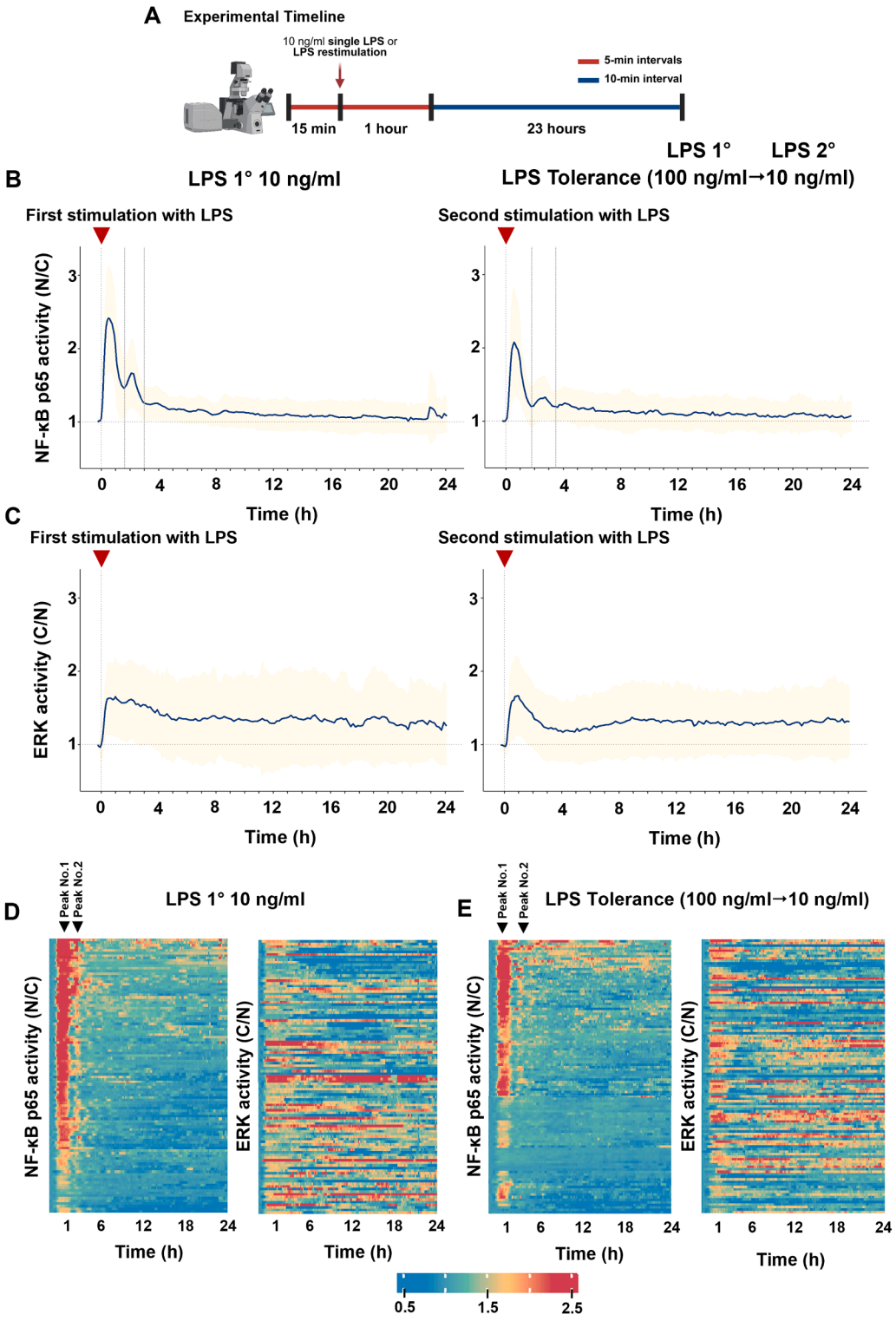

Fig. 2. Signaling dynamics of NF-κB p65 and ERK during single LPS stimulation and LPS tolerance (A) Experimental timeline indicated different time intervals during the experiment after a single LPS or LPS restimulation. (**B-C**) NF-κB p65 and ERK pathway reporter activities in RAW264.7 Trio cells subjected to either single LPS stimulation (10 ng/mL; $n = 104$ cells) or LPS tolerance ($n = 105$ cells; 100 ng/mL LPS followed by 10 ng/mL LPS) are shown as nuclear-to-cytoplasmic (N/C) and cytoplasmic-to-nuclear (C/N) ratios, respectively. The red arrow indicates the timing of LPS administration. The blue line represents the mean reporter activity, and the yellow shaded area indicates the standard error of the mean (SEM). Heatmap representations of single-cell NF-κB p65 and ERK reporter activities. Paired visualizations are shown for (**D**) LPS 1° 10 ng/ml and (**E**) LPS tolerance. Cells are sorted based on the NF-κB p65 activity, with identical row-ordering applied to the ERK activity to visualize coordinated responses. Black arrows indicated the first and second signal peaks.

time to first peak reflects the duration required to reach the initial peak response [37]. The results indicated that both the AUC and the amplitude features from ERK sensor in response to LPS 1° stimulation (10 ng/ml) were significantly greater than those observed in LPS tolerance ($p < 0.001$, Fig. 3**A** left and middle panels). Furthermore, the time to first peak of ERK signaling was significantly extended during LPS tolerance compared with primary LPS stimulation ($p < 0.01$), indicating a delayed initiation of ERK signaling in the tolerant state (Fig. 3**A** right panel).

Both the AUC and amplitude of NF-κB were higher following primary LPS stimulation (LPS 1°) than under LPS tolerance (Fig. 3**B**, left and middle panels), similar to the patterns observed for ERK signaling. In addition, similar to ERK signaling, the time to the first peak of NF-κB signaling was significantly extended in LPS-tolerant macrophages compared with single LPS stimulation ($p < 0.0001$) (Fig. 3**B**). In particular, to ensure that our observations in NF-κB signaling were not influenced by the transcriptional feedforward loop of the NF-κB reporter under the NF-κB p65 mouse promoter [38], we cross-validated the signaling characteristics by using the nuclear intensity of the NF-κB p65 sensor. The results correlated with the N/C ratio analysis, in which both the AUC and the amplitude significantly decreased in LPS tolerance compared to the primary LPS stimulation, and the time to first peak did not show a significant delay. This result confirmed that the hallmark of NF-κB signaling during LPS tolerance in our system was suppression of the response magnitude rather than an alteration in signaling kinetics (**Supplementary Figure S2A-C)**.

3.4. The crosstalk between ERK and Nf-κB pathways during LPS tolerance

In previous reports, the cross-talk between ERK and NF-κB signaling pathways was documented in macrophages stimulated with LPS, but such cross regulation has been poorly characterized in LPS tolerant state, especially in real-time at single-cell level [39–41]. To assess the crosstalk between these two pathways in LPS tolerance in macrophages, RAW264.7 Trio was treated with specific inhibitor following the stimulation scheme as depicted in Fig. 4**A**. The stimulation timeline began with seeding RAW264.7 Trio and primary stimulation at 100 ng/ml, followed by a 24-h rest period. Prior to the second stimulation, the specific inhibitor for ERK or NF-κB pathway was applied one hour before re-stimulation with 10 ng/ml of LPS. To suppress ERK signaling, PD98059 was used, which is a reversible MEK/ERK inhibitor whereas BAY 11–7082, was used as an NF-κB inhibitor. To exclude the potential cellular toxicity during the imaging session, the concentrations of selected inhibitors were tested for their effect on cell viability. The results showed that both the ERK inhibitor up to 100 μM **(Supplementary Figure S3A)** and the NF-κB inhibitor up to 5 μM **(Supplementary Figure S4A)** did not affect cell viability.

Next, we verified that the treatment of each inhibitor interfered with specific signaling pathway. RAW264.7 Trio were treated with an inhibitor one hour prior to 10 ng/ml LPS stimulation. Subsequently, after three hours, protein lysates were harvested and subjected to Western blot. Treatment of RAW264.7 Trio with increasing doses of ERK inhibitor clearly diminished the levels of ERK phosphorylation in a dose-dependent manner when compared to control ($p < 0.05$) **(Supplementary Figure S3B-C)**. Similarly, inhibition of NF-κB p65 led to a modest decrease in phosphorylation of both endogenous and exogenously overexpressed NF-κB p65, although the effect was not statistically significant (**Supplementary Figure S4B- S3D)**.

To examine the impact of each inhibitor on LPS tolerance phenotypes, IL-6 and TNFα secreted by RAW264.7 Trio under inhibitor treatment were detected by ELISA as depicted in Fig. 4**A**. Six hours of post-stimulation, the cultured supernatant was harvested for ELISA. Addition of an ERK inhibitor further suppressed IL-6 production compared with the mock-treated LPS tolerance control ($p < 0.0001$). In

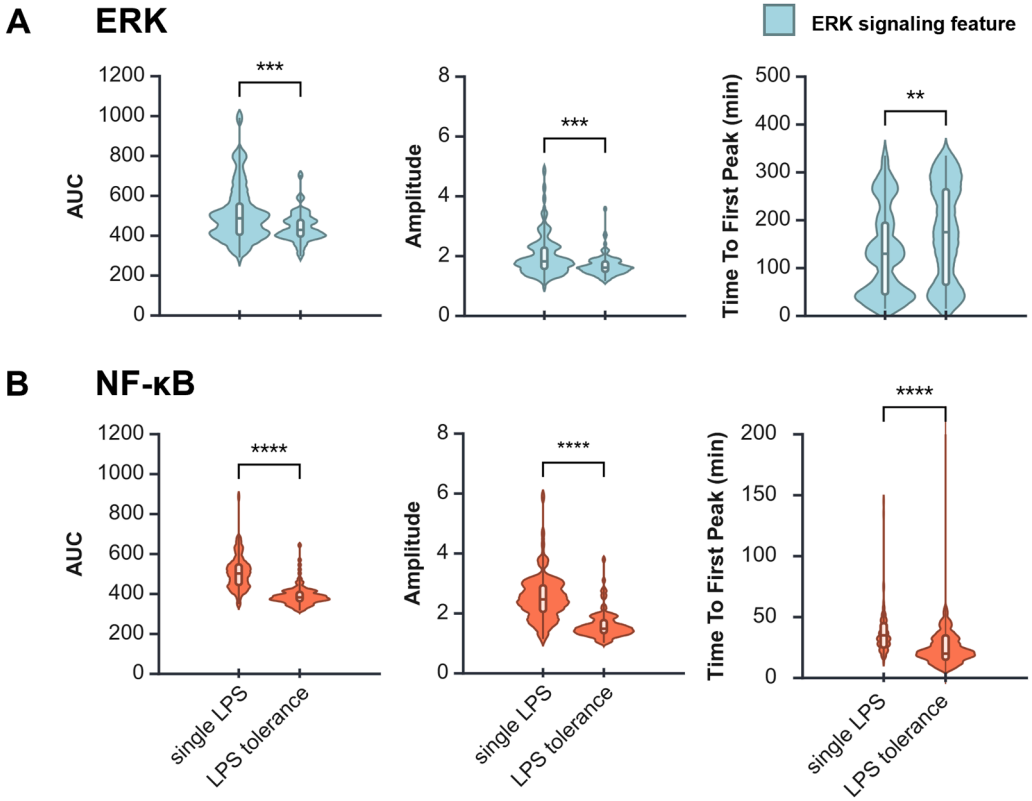

Fig. 3. The signaling features for ERK and NF-κB p65 pathways during LPS stimulation and LPS tolerance (A) ERK and (**B**) NF-κB p65 signaling features, including area under the curve (AUC), amplitude, and time to first peak, are shown. **, ***, and **** indicate significant differences at $p < 0.01$, $p < 0.001$, and $p < 0.0001$, respectively (unpaired Mann–Whitney U test). For details in image processing, please refer to Fig. 2 and Materials and Methods.

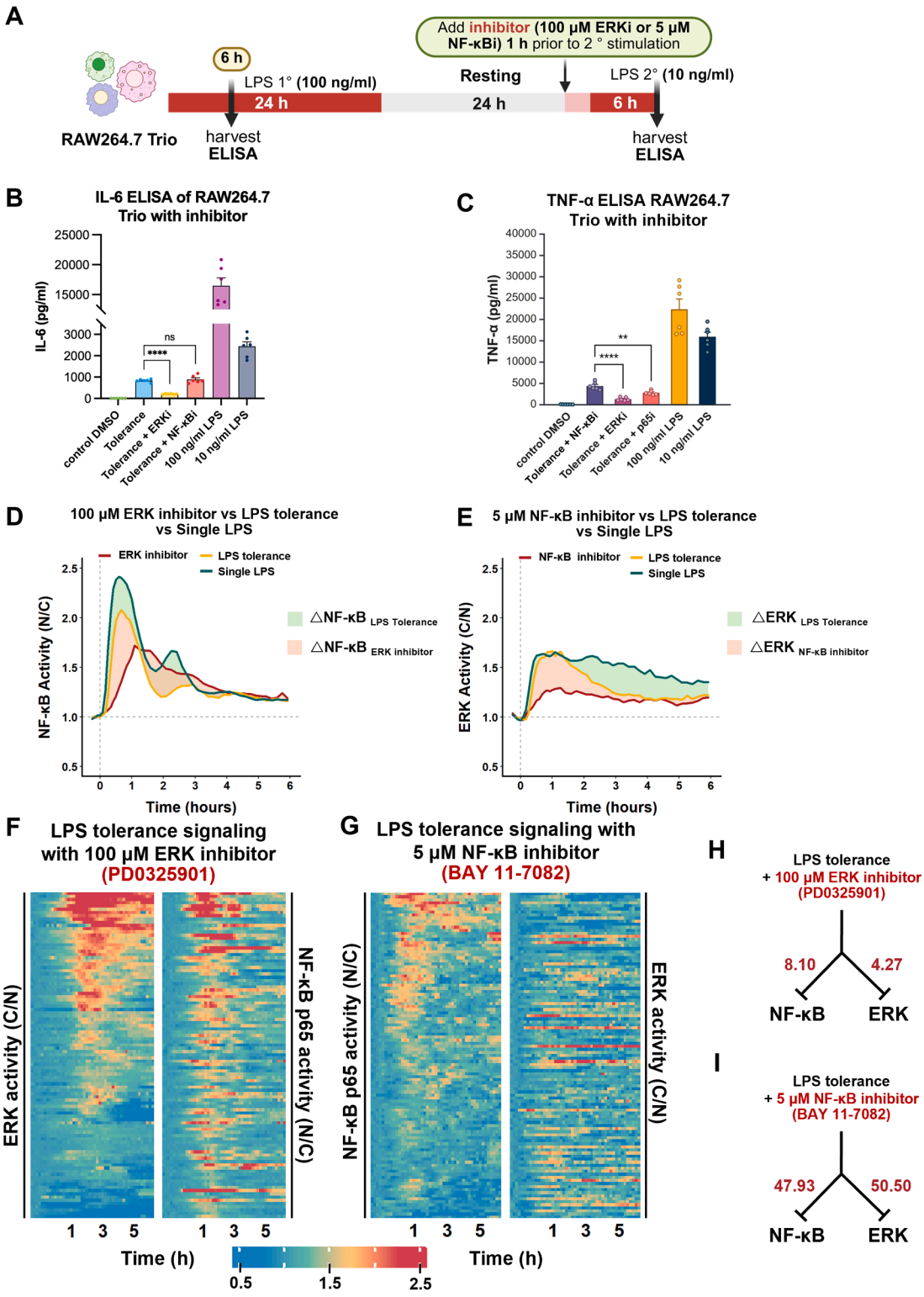

Fig. 4. Impact of specific inhibitors on the signaling dynamics during LPS tolerance and the crosstalk between the ERK and NF-κB signaling pathways (A) Schematic timeline illustrating inhibitor treatment and LPS stimulation protocol. (B-C) IL-6 and TNF-α production at 6 h after LPS re-stimulation in the presence or absence of inhibitors. **** indicates significant differences at $p < 0.0001$, and n.s. indicates no statistically significant difference, as determined by one-way ANOVA with Dunnett's multiple-comparison test. (D) NF-κB p65 (N/C ratio) and (E) ERK (C/N ratio) under three conditions: Single LPS (green), LPS tolerance (orange), and LPS tolerance with the addition of a specific inhibitor (red; ERK inhibitor in D and NF-κB inhibitor in E) monitoring for 6 h. The brackets (△) indicated the difference between LPS tolerance compared to a single LPS stimulation and the difference between LPS tolerance and LPS tolerance with a specific inhibitor. Heatmap representations of LPS tolerance NF-κB p65 and ERK reporter activities. Paired visualizations are shown for LPS tolerance signaling with (**F**) ERK inhibitor (PD0325901) and (**G**) NF-κB inhibitor (BAY 11–7082). (H-I) Schematic illustrating cross-inhibitory effects of ERK and NF-κB inhibitor pretreatment during LPS tolerance. The concentrations of each inhibitor used in these experiments were 100 μM for the ERK inhibitor (PD0325901) and 5 μM for the NF-κB inhibitor (BAY 11–7082), as indicated.

contrast, inhibition of NF-κB p65 did not produce a detectable effect on IL-6 levels relative to the mock-treated LPS-tolerant group (Fig. 4**B**). TNF-α production was subsequently assessed and revealed that both ERK and NF-κB p65 inhibitors significantly further reduced TNF-α levels under LPS-tolerant conditions ($p < 0.0001$ and $p < 0.01$, respectively), compared with the mock-treated tolerance control (Fig. 4**C**). Collectively, these data suggest that ERK signaling may preferentially contribute to IL-6 regulation during LPS tolerance, while both ERK and NF-κB p65 pathways appear to be involved in modulating TNF-α production under tolerant conditions.

We next investigated pathway crosstalk by quantifying the relative contribution of each pathway to cross-inhibition under LPS tolerant conditions. When ERK signaling pathway was inhibited, the signaling dynamic of NF-κB was dampened and delayed, as observed by fewer peak numbers and delayed time to first peak. (Fig. 4**D**). On the other hand, the ERK activity was also dampened by NF-κB inhibition in LPS tolerized macrophages (Fig. 4**E**). To monitor cross-inhibition at the single-cell level, the paired heatmaps showed that the inhibitor effectively blocked specific signaling pathway. ERK inhibitor (PD0325901) treatment revealed that the inhibitor has only a limited impact on ERK activity, while the NF-κB activity remained robustly detectable within the same individual cells (Fig. 4**F**). On the contrary, treatment with NF-κB inhibitor (BAY 11-7082) showed that the inhibitor almost completely suppressed NF-κB activity. Moreover, the effect of NF-κB inhibition on ERK signaling was greater than that of an ERK inhibitor (Fig. 4**F, G**). The paired heatmap indicated an asymmetric crosstalk between the two pathways, in which ERK inhibition minimally interfered with the NF-κB signaling pathway, whereas NF-κB inhibition exerted a profound cross-inhibitory effect on ERK dynamics.

To quantify the crosstalk between NF-κB and ERK signaling, we measured the integrated signaling output over 6 h based on the average AUC for each condition (Fig. 4**D**). We first determined the extent to which LPS tolerance suppresses these signaling pathways by calculating the cumulative activity loss between the single LPS stimulation and the LPS-tolerized states, as indicated below.

$$\triangle \text{NF-κB}_{\text{ Tolerance}} = \text{NF-κB}_{\text{ AUC Single LPS}} - \text{NF-κB}_{\text{ AUC LPS Tolerance}}$$

This quantification revealed a tolerance-induced attenuation of 46.39 (**Supplementary Figure S4E**, left side). Within these tolerant macrophages, we further assessed the dependence of the residual NF-κB signal on the ERK activity upon treatment with an ERK inhibitor using the following formula.

$$\triangle \text{NF-κB}_{\text{ ERK inhibitor}} = \text{NF-κB}_{\text{ AUC LPS Tolerance}} - \text{NF-κB}_{\text{ AUC ERK inhibitor}}$$

Under the LPS tolerant conditions, ERK inhibition resulted in a substantial integrated signaling output loss of NF-κB at 8.10 (Fig. 4**H**, left side). A reciprocal analysis was performed to evaluate the impact of LPS tolerance and NF-κB signaling on ERK activity. We measured the cumulative changes in ERK integrated signaling output over 6 h. (Fig. 4**E**). Next, we determined the total ERK activity loss under the tolerance condition using the following formula.

$$\triangle \text{ERK}_{\text{ Tolerance}} = \text{ERK}_{\text{ AUC Single LPS}} - \text{ERK}_{\text{ AUC LPS Tolerance}}$$

The induction of LPS tolerance caused a substantial reduction in the ERK activity of 59.11 (**Supplementary Figure S4E**, right side). Next, we assessed the effect of blockade of NF-κB on ERK activity in the tolerant cells using the following formula.

$$\triangle \text{ERK}_{\text{ NF-kB inhibitor}} = \text{ERK}_{\text{ AUC LPS Tolerance}} - \text{ERK Activity}_{\text{ AUC inhibitor}}$$

This calculation yielded a profound reduction of ERK signal of 50.50 (Fig. 4**I**, right side). Collectively, these quantitative measurements demonstrated that NF-κB represents a directional regulator of ERK dynamics under LPS tolerance conditions, while ERK signaling has a marginal effect on NF-κB activity.

4. Discussion

In this study, we investigated the effect of LPS tolerance on the dynamics of two key inflammatory signaling pathways, NF-κB and ERK, using macrophage cell line engineered to stably express ERK KTR Clover [22] and NF-κB p65 mRuby2 [24]. This reporter cell enables the real-time detection of the key signaling events at single-cell level. Single-dose LPS stimulation induced a robust production of pro-inflammatory cytokines TNF-α and IL-6 at transcriptional and protein levels, as expected [42–44]. This induction occurs in macrophages through well-established LPS/TLR4/MyD88/TRIF-mediated signaling cascade that culminates in the activation of NF-κB [42,45,46] and ERK MAPK signaling pathways [43,45,46]. More importantly, we observed at the single-cell level the characteristic of NF-κB oscillations in response to LPS that is initiated by a peak with high magnitude, followed by multiple, smaller magnitude peaks. The first peak potentially represents a MyD88-mediated activation of the NF-κB p65 while the subsequent smaller peaks are potentially mediated by TRIF signaling, which leads to a delayed negative feedback loop involving IκB-alpha [22,24]. Our findings on NF-κB signaling dynamics correlate with previous studies, demonstrating that the initial activation peak following LPS stimulation occurs within a similar timeframe, with the subsequent second peak likewise corroborating existing literature [24,47].

In addition to NF-κB signaling, we observed a sustained increase in ERK activity following a single-dose LPS stimulation. The activation of ERK is known to diverge from TLR4 signaling through TAK1/IκB-alpha axis, leading to a TPL-2-mediated degradation of NF-κB p105 [21,48]. The signal from ERK MAPK pathway is required to enhance NF-κB-mediated gene expression, particularly when macrophages are stimulated with low concentrations of LPS such as from the commensal bacteria [49–54]. The findings on ERK activity are similar to a previous study that reported on p38 signaling dynamics, which are part of the MAPK family that is stimulated with LPS, exhibiting peaks that ascend, descend, and then sustain [21]. This parallels the expected response, as both pathways are regulated by identical upstream signaling components [55].

Under LPS-tolerant conditions, single-cell analysis revealed distinct alterations in signaling dynamics, including a delayed time to the first peak and reduced magnitude of subsequent NF-κB oscillations, together with a transient attenuation of ERK activity. These observations suggest that cellular signaling dynamics are altered during the development of LPS tolerance. These findings are consistent with the possibility that inhibitory events at proximal signaling steps influence the observed kinetic delay. Mechanistically, the kinetic delay of signaling may result from the up-regulation and/or increased recruitment of IRAK-M (IL-1 Receptor-Associated Kinase-M) to the MyD88 signaling complex. IRAK-M acts as a negative regulator of TLR signaling by impeding the phosphorylation and dissociation of IRAK-1/4, which are required to activate downstream signaling cascades such as MAPK and NF-κB. This interference creates molecular bottleneck, forcing individual cells to overcome a higher activation threshold. Previous studies have suggested that IRAK-M$^{-/-}$ macrophages show increased cytokine production, such as IL-6 and TNF-α, compared to wild-type control [56], emphasizing the essential function of IRAK-M in attenuating TLR4 signaling, which likely accounts for the delayed kinetics we found. Upregulation of IRAK-M is shown to be associated with LPS tolerance in human endotoxemia model [57].

The transient dampening of ERK activity seen at the single-cell level is corroborated by a reduction in ERK phosphorylation previously demonstrated via immunoblotting in LPS-tolerant BMDM [58]. However, the specific mechanism controlling ERK activity in LPS tolerance remains poorly understood. For example, DOK3 is reported as a negative regulator of ERK in LPS-stimulated macrophages [59]. Its consistently higher expression during LPS tolerance may not fully account for the subtle distinctions we observed, such as increased response heterogeneity. Despite these dampening effects, analyses of gene expression

profiles in macrophages rendered tolerant by CpG, PolyI:C, or LPS priming all show an enrichment in NF-κB and MAPK signaling components, in addition to changes in NF-κB oscillations and open chromatin accessibility [25].

Among the key regulators of LPS/TLR4 signaling, phosphatases play crucial roles in attenuating signal transduction downstream of TLR4 during LPS tolerance [60]. Several phosphatases, including PP1, PP2A, SHIP and dual-specificity phosphatases (DUSPs) dephosphorylate components of the MAPK and NF-κB pathways, thereby limiting the duration and amplitude of signaling [61–63]. Upregulation of these phosphatases during LPS tolerance contributes to the suppression of proinflammatory cytokine production and the maintenance of a refractory state. Thus, phosphatase-mediated negative regulation represents an essential mechanism that fine-tunes inflammatory signaling and ensures resolution of the immune response upon repeated LPS exposure. The blunted signaling dynamics observed in our study are possibly the impact of these negative regulators.

In this study, the signal dynamics were investigated in RAW264.7 cell line which are cultured in a monolayer. During the early phase of activation, the influence of paracrine signaling from neighboring cells, such as the TNF-α feedback loop, is expected to be minimal [38]. However, over longer observation periods, the contribution of secondary effects mediated by factors secreted from neighboring cells cannot be excluded. Therefore, the long-term effects observed in this study may partly reflect secondary responses induced by paracrine factors, which could vary depending on the spatial positioning of individual cells.

To delineate the crosstalk between NF-κB and ERK signaling pathways, we conducted pharmacological inhibition experiments. First, blocking the ERK signal with the reversible ERK inhibitor PD0325901 altered NF-κB activity in LPS tolerant macrophages; it resulted in a single peak and a delayed response time compared to LPS tolerant cells without inhibitor. This observation suggests that ERK signaling has a minimal effect on the overall NF-κB response. A recent study further supports this observation, showing that macrophages pretreated with an ERK inhibitor exhibited reduced p65 phosphorylation [41] as well as diminished production of pro-inflammatory cytokines [40]. However, study in human monocyte THP-1 treated with PD0325901 prior to LPS stimulation reported no change in DNA binding of NF-κB p65 but a slight inhibition of nuclear translocation [64].

Second, blocking NF-κB signaling in LPS tolerant macrophages inhibited not only NF-κB but also ERK activity. This result aligns with the findings that NF-κB inhibition can suppress ERK and other pathways, including AP-1, Akt, and PI3K, in LPS-stimulated macrophages [39]. Finally, quantitation of cross-inhibition revealed that LPS tolerance negatively inhibits ERK activity at a greater AUC reduction than NF-κB activity. In the LPS tolerant state, the crosstalk between NF-κB and ERK signaling pathways is most profound when the NF-κB signal is abolished, as evidenced by a strong cross-inhibition on ERK activity, a delayed time to first peak, and a flattened signaling curve. Collectively, these results support the conclusion that NF-κB signaling is required to fine-tune the ERK-mediated inflammatory response in LPS-tolerant macrophages.

A limitation of our study is the use of an NF-κB p65–mRuby2 fusion protein as a reporter for NF-κB activity, which may potentially interfere with endogenous NF-κB signaling. In addition, our assessment of LPS tolerance relied on pharmacological inhibition of ERK and NF-κB pathways; as these chemical inhibitors may induce cytotoxic effects with prolonged exposure beyond 6 h. Future studies should further examine the impact of ERK inhibition on NF-κB signaling within the context of TLR4 signal transduction, including the involvement of MyD88- and TRIF-dependent pathways. These findings may contribute to a better understanding of how temporal features of macrophage signaling such as timing, amplitude, and oscillatory behavior are altered during LPS tolerance, based on insights gained from pathway inhibition studies.

5. Conclusions

This study reveals a quantitative analysis of the signaling dynamics of ERK and NF-κB p65 under LPS tolerance conditions in macrophages. From single-cell live-cell imaging, we demonstrated that both ERK and NF-κB p65 signaling under LPS tolerance exhibited reduced AUC and amplitude. Furthermore, the initial response was significantly delayed in the LPS tolerance group compared to single LPS stimulation. For cross-regulation between ERK and NF-κB, blocking ERK altered NF-κB signaling, and NF-κB inhibition suppressed ERK dynamics that emphasize a highly linked and interdependent signaling network. These LPS tolerance signaling dynamics may shape future strategies to prevent immune paralysis while preserving host defense in clinical conditions such as sepsis and chronic infection.

CRediT authorship contribution statement

Tuntikorn Laosuk: Writing – review & editing, Writing – original draft, Visualization, Methodology, Investigation, Formal analysis, Data curation, Conceptualization. **Patipark Kueanjinda:** Writing – original draft, Resources, Methodology, Conceptualization. **Hiroshi Kimura:** Resources, Methodology, Investigation, Data curation, Conceptualization. **Tanapat Palaga:** Writing – review & editing, Writing – original draft, Validation, Supervision, Project administration, Methodology, Funding acquisition, Data curation, Conceptualization.

Declaration of competing interest

All authors declare no competing interests.

Acknowledgements

This research project is supported by the Second Century Fund (C2F), Chulalongkorn University and the 90th Anniversary of Chulalongkorn University Scholarship under the Ratchadapisek Somphot Endowment Fund. This project is supported in part by the NSRF via the Program Management Unit for Human Resources & Institutional Development, Research and Innovation (Grant No. B16F640117), Thailand Science research and Innovation Fund Chulalongkorn University (HEA_FF_69_110_2300_028) and by National Research Council of Thailand (NRCT) and Chulalongkorn University (N42A680063).

Supplementary materials

Supplementary material associated with this article can be found, in the online version, at doi:10.1016/j.btre.2026.e00966.

Data availability

Data will be made available on request.

References

[1] S.E. Turvey, D.H. Broide, Innate immunity, J. Allergy Clin. Immunol. 125 (2 Suppl 2) (2010) S24–S32.
[2] M.G. Netea, L.A. Joosten, E. Latz, K.H. Mills, G. Natoli, H.G. Stunnenberg, et al., Trained immunity: a program of innate immune memory in health and disease, Science (1979) 352 (6284) (2016) aaf1098.
[3] P. Vuscan, B. Kischkel, L.A.B. Joosten, M.G. Netea, Trained immunity: general and emerging concepts, Immunol. Rev. 323 (1) (2024) 164–185.
[4] M. Sadeghi, M. Divangahi, Discovering adaptive features of innate immune memory, Immunol. Rev. 323 (1) (2024) 186–196.
[5] T. Lajqi, N. Kostlin-Gille, R. Bauer, S.G. Zarogiannis, E. Lajqi, V. Ajeti, et al., Training vs. Tolerance: the yin/yang of the Innate Immune System, Biomedicines 11 (3) (2023) 766.
[6] S.K. Biswas, E. Lopez-Collazo, Endotoxin tolerance: new mechanisms, molecules and clinical significance, Trends Immunol. 30 (10) (2009) 475–487.
[7] S.L. Foster, D.C. Hargreaves, R. Medzhitov, Gene-specific control of inflammation by TLR-induced chromatin modifications, Nature 447 (7147) (2007) 972–978.

[8] M. Divangahi, P. Aaby, S.A. Khader, L.B. Barreiro, S. Bekkering, T. Chavakis, et al., Author correction: trained immunity, tolerance, priming and differentiation: distinct immunological processes, Nat. Immunol. 22 (7) (2021) 928.

[9] J.J. Seeley, S. Ghosh, Molecular mechanisms of innate memory and tolerance to LPS, J. Leukoc. Biol. 101 (1) (2017) 107–119.

[10] Y. Cheng, T.N. Marion, X. Cao, W. Wang, Y. Cao, Park 7: a novel therapeutic target for macrophages in sepsis-induced immunosuppression, Front. Immunol. 9 (2018) 2632.

[11] W. Wang, L. Ma, B. Liu, L. Ouyang, The role of trained immunity in sepsis, Front. Immunol. 15 (2024) 1449986.

[12] J. Gillen, T. Ondee, D. Gurusamy, J. Issara-Amphorn, N.P. Manes, S.H. Yoon, et al., LPS tolerance inhibits cellular respiration and induces global changes in the macrophage secretome, Biomolecules 11 (2) (2021) 164.

[13] K. Chen, S. Geng, R. Yuan, N. Diao, Z. Upchurch, L. Li, Super-low dose endotoxin pre-conditioning exacerbates sepsis mortality, EBioMedicine 2 (4) (2015) 324–333.

[14] R.M. Lucas, L. Luo, J.L. Stow, ERK1/2 in immune signalling, Biochem. Soc. Trans. 50 (5) (2022) 1341–1352.

[15] T. Kawai, S. Akira, Signaling to NF-kappaB by toll-like receptors, Trends Mol. Med. 13 (11) (2007) 460–469.

[16] L. Luo, R.M. Lucas, L. Liu, J.L. Stow, Signalling, sorting and scaffolding adaptors for toll-like receptors, J. Cell Sci. 133 (5) (2020) jcs239194.

[17] K. Lane, D. Van Valen, M.M. DeFelice, D.N. Macklin, T. Kudo, A. Jaimovich, et al., Measuring signaling and RNA-seq in the same cell links gene expression to dynamic patterns of NF-kappaB activation, Cell Syst. 4 (4) (2017) 458–469.e5, e5.

[18] T.K. Lee, E.M. Denny, J.C. Sanghvi, J.E. Gaston, N.D. Maynard, J.J. Hughey, et al., A noisy paracrine signal determines the cellular NF-κb response to lipopolysaccharide, Sci. Signal. 2 (93) (2009) ra65, ra.

[19] S. Zambrano, I. De Toma, A. Piffer, M.E. Bianchi, A. Agresti, NF-kappaB oscillations translate into functionally related patterns of gene expression, Elife 5 (2016) e09100.

[20] M. Son, T. Frank, T. Holst-Hansen, A.G. Wang, M. Junkin, S.S. Kashaf, et al., Spatiotemporal NF-kappaB dynamics encodes the position, amplitude, and duration of local immune inputs, Sci. Adv. 8 (35) (2022) eabn6240.

[21] S. Luecke, X. Guo, K.M. Sheu, A. Singh, S.C. Lowe, M. Han, et al., Dynamical and combinatorial coding by MAPK p38 and NFkappaB in the inflammatory response of macrophages, Mol. Syst. Biol. 20 (8) (2024) 898–932.

[22] T. Kudo, S. Jeknic, D.N. Macklin, S. Akhter, J.J. Hughey, S. Regot, et al., Live-cell measurements of kinase activity in single cells using translocation reporters, Nat. Protoc. 13 (1) (2018) 155–169.

[23] S. Regot, J.J. Hughey, B.T. Bajar, S. Carrasco, M.W. Covert, High-sensitivity measurements of multiple kinase activities in live single cells, Cell 157 (7) (2014) 1724–1734.

[24] K. Lane, M. Andres-Terre, T. Kudo, D.M. Monack, M.W. Covert, Escalating threat levels of bacterial infection can Be discriminated by distinct MAPK and NF-kappaB signaling dynamics in single host cells, Cell Syst. 8 (3) (2019) 183–196.e4, e4.

[25] A.G. Wang, M. Son, A. Gorin, E. Kenna, A. Padhi, B. Keisham, et al., Macrophage memory emerges from coordinated transcription factor and chromatin dynamics, Cell Syst. 16 (2) (2025) 101171.

[26] B. Novakovic, E. Habibi, S.Y. Wang, R.J.W. Arts, R. Davar, W. Megchelenbrink, et al., beta-glucan reverses the epigenetic State of LPS-induced immunological tolerance, Cell 167 (5) (2016) 1354–1368.e14, e14.

[27] S. Chen, J. Yang, Y. Wei, X. Wei, Epigenetic regulation of macrophages: from homeostasis maintenance to host defense, Cell Mol. Immunol. 17 (1) (2020) 36–49.

[28] S. Benjaskulluecha, A. Boonmee, T. Pattarakankul, B. Wongprom, J. Klomsing, T. Palaga, Screening of compounds to identify novel epigenetic regulatory factors that affect innate immune memory in macrophages, Sci. Rep. 12 (1) (2022) 1912.

[29] E. Lopez-Collazo, C. Del Fresno, Endotoxin tolerance and trained immunity: breaking down immunological memory barriers, Front. Immunol. 15 (2024) 1393283.

[30] F. Pankratz, X. Bemtgen, R. Zeiser, F. Leonhardt, S. Kreuzaler, I. Hilgendorf, et al., MicroRNA-155 exerts cell-specific antiangiogenic but proarteriogenic effects during adaptive neovascularization, Circulation 131 (18) (2015) 1575–1589.

[31] T. Francetic, M. Le May, M. Hamed, H. Mach, D. Meyers, P.A. Cole, et al., Regulation of Myf5 early enhancer by histone acetyltransferase p300 during stem cell differentiation, Mol. Biol. 01 (2012).

[32] S. Beinke, M.J. Robinson, M. Hugunin, S.C. Ley, Lipopolysaccharide activation of the TPL-2/MEK/extracellular signal-regulated kinase mitogen-activated protein kinase cascade is regulated by IkappaB kinase-induced proteolysis of NF-kappaB1 p105, Mol. Cell Biol. 24 (21) (2004) 9658–9667.

[33] celltracking [Internet], https://github.com/hengkp/celltracking/releases/tag/v1.0.2, 2022.

[34] D.R. Stirling, M.J. Swain-Bowden, A.M. Lucas, A.E. Carpenter, B.A. Cimini, A. Goodman, CellProfiler 4: improvements in speed, utility and usability, BMC Bioinform. 22 (1) (2021) 433.

[35] L. Kamentsky, T.R. Jones, A. Fraser, M.A. Bray, D.J. Logan, K.L. Madden, et al., Improved structure, function and compatibility for CellProfiler: modular high-throughput image analysis software, Bioinformatics 27 (8) (2011) 1179–1180.

[36] H. Miura, Y. Kondo, M. Matsuda, K. Aoki, Cell-to-Cell heterogeneity in p38-mediated cross-inhibition of JNK causes stochastic Cell death, Cell Rep. 24 (10) (2018) 2658–2668.

[37] S.M.T. Rahman, M. Aqdas, E.W. Martin, F. Tomassoni Ardori, P. Songkiatisak, K. S. Oh, et al., Double knockin mice show NF-kappaB trajectories in immune signaling and aging, Cell Rep. 41 (8) (2022) 111682.

[38] M.H. Sung, N. Li, Q. Lao, R.A. Gottschalk, G.L. Hager, I.D. Fraser, Switching of the relative dominance between feedback mechanisms in lipopolysaccharide-induced NF-kappaB signaling, Sci. Signal. 7 (308) (2014) ra6.

[39] J. Lee, M.H. Rhee, E. Kim, J.Y. Cho, BAY 11-7082 is a broad-spectrum inhibitor with anti-inflammatory activity against multiple targets, Mediators Inflamm. 2012 (2012) 1–11.

[40] M. De, G. Serpa, E. Zuiker, K.B. Hisert, W.C. Liles, A.M. Manicone, et al., MEK1/2 inhibition decreases pro-inflammatory responses in macrophages from people with cystic fibrosis and mitigates severity of illness in experimental murine methicillin-resistant Staphylococcus aureus infection, Front. Cell Infect. Microbiol. 14 (2024) 1275940.

[41] T. Jiang, Y. Gong, W. Zhang, J. Qiu, X. Zheng, Z. Li, et al., PD0325901, an ERK inhibitor, attenuates RANKL-induced osteoclast formation and mitigates cartilage inflammation by inhibiting the NF-kappaB and MAPK pathways, Bioorg. Chem. 132 (2023) 106321.

[42] X. Liu, S. Yin, Y. Chen, Y. Wu, W. Zheng, H. Dong, et al., LPS-induced proinflammatory cytokine expression in human airway epithelial cells and macrophages via NF-κb, STAT3 or AP-1 activation, Mol. Med. Rep. 17 (4) (2018) 5484–5491.

[43] J.S. Cho, J.H. Kang, J.Y. Um, I.H. Han, I.H. Park, H.M. Lee, Lipopolysaccharide induces pro-inflammatory cytokines and MMP production via TLR4 in nasal polyp-derived fibroblast and organ culture, PLoS One 9 (11) (2014) e90683.

[44] M. Guha, M.A. O'Connell, R. Pawlinski, A. Hollis, P. McGovern, S.-F. Yan, et al., Lipopolysaccharide activation of the MEK-ERK1/2 pathway in human monocytic cells mediates tissue factor and tumor necrosis factor α expression by inducing Elk-1 phosphorylation and Egr-1 expression: presented in abstract form at the 42nd annual meeting of the American Society of Hematology, December 1-5, 2000, San Francisco, CA, Blood 98 (5) (2001) 1429–1439.

[45] X. Li, M. Xu, J. Shen, Y. Li, S. Lin, M. Zhu, et al., Sorafenib inhibits LPS-induced inflammation by regulating lyn-MAPK-NF-kB/AP-1 pathway and TLR4 expression, Cell Death Discov. 8 (1) (2022) 281.

[46] W. Zhao, H. Wang, C. Dai, B. Li, Y. Fu, J. Cheng, et al., The Erk1/2-EGR1 signaling pathway is involved in lipopolysaccharide-induced transforming growth factor-beta 1 expression in mouse macrophages, Microb. Pathog. 203 (2025) 107453.

[47] J. Sakai, E. Cammarota, J.A. Wright, P. Cicuta, R.A. Gottschalk, N. Li, et al., Lipopolysaccharide-induced NF-kappaB nuclear translocation is primarily dependent on MyD88, but TNFalpha expression requires TRIF and MyD88, Sci. Rep. 7 (1) (2017) 1428.

[48] A. Banerjee, S. Gerondakis, Coordinating TLR-activated signaling pathways in cells of the immune system, Immunol. Cell Biol. 85 (6) (2007) 420–424.

[49] M.C. Abt, L.C. Osborne, L.A. Monticelli, T.A. Doering, T. Alenghat, G. F. Sonnenberg, et al., Commensal bacteria calibrate the activation threshold of innate antiviral immunity, Immunity 37 (1) (2012) 158–170.

[50] T.B. Clarke, K.M. Davis, E.S. Lysenko, A.Y. Zhou, Y. Yu, J.N. Weiser, Recognition of peptidoglycan from the microbiota by Nod1 enhances systemic innate immunity, Nat. Med 16 (2) (2010) 228–231.

[51] S.C. Ganal, S.L. Sanos, C. Kallfass, K. Oberle, C. Johner, C. Kirschning, et al., Priming of natural killer cells by nonmucosal mononuclear phagocytes requires instructive signals from commensal microbiota, Immunity 37 (1) (2012) 171–186.

[52] R.A. Gottschalk, A.J. Martins, B.R. Angermann, B. Dutta, C.E. Ng, S. Uderhardt, et al., Distinct NF-kappaB and MAPK activation thresholds uncouple steady-State microbe sensing from anti-pathogen inflammatory responses, Cell Syst. 2 (6) (2016) 378–390.

[53] N. Iida, A. Dzutsev, C.A. Stewart, L. Smith, N. Bouladoux, R.A. Weingarten, et al., Commensal bacteria control cancer response to therapy by modulating the tumor microenvironment, Science (1979) 342 (6161) (2013) 967–970.

[54] C.J. Kelly, S.P. Colgan, D.N. Frank, Of microbes and meals: the health consequences of dietary endotoxemia, Nutr. Clin. Pract. 27 (2) (2012) 215–225.

[55] S. Akira, K. Takeda, Toll-like receptor signalling, Nat. Rev. Immunol. 4 (7) (2004) 499–511.

[56] K. Kobayashi, L.D. Hernandez, J.E. Galan, C.A. Janeway Jr., R. Medzhitov, R. A Flavell, IRAK-M is a negative regulator of toll-like receptor signaling, Cell 110 (2) (2002) 191–202.

[57] C. van 't Veer, P.S. van den Pangaart, M.A. van Zoelen, M. de Kruif, R.S. Birjmohun, E.S. Stroes, et al., Induction of IRAK-M is associated with lipopolysaccharide tolerance in a human endotoxemia model, J. Immunol. 179 (10) (2007) 7110–7120.

[58] A. Boonmee, S. Benjaskulluecha, P. Kueanjinda, B. Wongprom, T. Pattarakankul, T. Palaga, The chemotherapeutic drug carboplatin affects macrophage responses to LPS and LPS tolerance via epigenetic modifications, Sci. Rep. 11 (1) (2021) 21574.

[59] Q. Peng, J.L. O'Loughlin, M.B Humphrey, DOK3 negatively regulates LPS responses and endotoxin tolerance, PLoS One 7 (6) (2012) e39967.

[60] C.H.T. Seumen, T.M. Grimm, C.R. Hauck, Protein phosphatases in TLR signaling, Cell Commun. Signal. 19 (1) (2021) 45.

[61] L. Sun, A.L. Ii, T.T. Pham, T.P. Shanley, Study of protein phosphatase 2A (PP2A) activity in LPS-induced tolerance using fluorescence-based and immunoprecipitation-aided methodology, Biomolecules 5 (3) (2015) 1284–1301.

[62] Y. Xiong, A.E. Medvedev, Induction of endotoxin tolerance in vivo inhibits activation of IRAK4 and increases negative regulators IRAK-M, SHIP-1, and A20, J. Leukoc. Biol. 90 (6) (2011) 1141–1148.

[63] L.M. Sly, M.J. Rauh, J. Kalesnikoff, C.H. Song, G. Krystal, LPS-induced upregulation of SHIP is essential for endotoxin tolerance, Immunity 21 (2) (2004) 227–239.

[64] M. Guha, M.A. O'Connell, R. Pawlinski, A. Hollis, P. McGovern, S.F. Yan, et al., Lipopolysaccharide activation of the MEK-ERK1/2 pathway in human monocytic cells mediates tissue factor and tumor necrosis factor alpha expression by inducing Elk-1 phosphorylation and egr-1 expression, Blood 98 (5) (2001) 1429–1439.